Improvement of lake ice thickness retrieval from MODIS satellite data using a thermodynamic model

Homa Kheyrollah Pour[1,2], Claude R. Duguay[1], K. Andrea Scott[3], Kyung-Kuk Kang[1]

[1]Department of Geography and Environmental Management, University of Waterloo, Waterloo, Ontario, Canada
[2]Environment and Climate Change Canada, 4905 Dufferin Street, Toronto, Ontario, Canada
[3]Department of System Design Engineering, University of Waterloo, Waterloo, Ontario, Canada
(Corresponding author e-mail: h2kheyro@uwaterloo.ca)

Abstract- **Observations of ice thickness are limited in high latitude regions, at a time when they are increasingly being requested by operational ice centers. This study aims to improve the retrieval of lake ice thickness using data from the Moderate Resolution Imaging Spectroradiometer (MODIS) on board NASA's Aqua (PM) and Terra (AM) satellites. The accuracy of ice thickness retrievals based on MODIS Lake Ice Surface Temperature (LIST) is investigated using a commonly used heat balance equation and the retrieved ice thicknesses are compared to in-situ measurements from the Canadian Ice Service. The accuracy of ice thickness estimates is improved when using snow depth from a 1-D thermodynamic lake ice model CLIMo (Canadian Lake Ice Model) rather than an empirical relationship between snow depth and ice thickness utilized in recent investigations. Taking into account all data over the study period (2002-2014) the mean bias error and the root mean square error are reduced from -0.42 m to 0.07 m and 0.58 m to 0.17 m, respectively with the novel approach proposed herein. However, this approach is limited to ice thickness estimations of less than ca. 1.7 m.**

***Index Terms* – Ice thickness, MODIS, Lake ice, Lake ice model, Lake surface temperature.**

I. INTRODUCTION

Knowledge of the thickness of sea or lake ice and the overlying snow cover is an important requirement when addressing interactions between the sea or lake and the atmosphere during winter at high latitudes. In particular, ice thickness and snow depth over seas and inland water bodies impact the heat flux from the relatively warm water to the cold atmosphere **[1]**. The heterogeneity of ice thickness and depth of snow on ice leads to variations in thermal properties of the ice and snow, which in turn lead to variations in the heat flux **[2]**. Estimation of the heat exchange between the sea/lake and the atmosphere, which is essential in numerical weather prediction and climate modeling, requires accurate information of ice thickness and on-ice snow depth.

Despite the above noted requirement, knowledge about sea/lake ice thickness around the globe is remarkably limited. This is mainly due to difficulties in collecting measurements of ice thickness directly in the field, particularly in the Arctic (i.e. remoteness of sites and costs associated with field deployments). To overcome this problem, a series of methods have been developed to infer ice thickness using satellite data. For example, sea ice thickness has been estimated from measurements of sea ice freeboard obtained using radar and laser altimeters, although the relative errors are large for ice of thickness less than 1.0 m **[3-7]**. Passive microwave radiometer data obtained at various frequencies (19, 37, and 85 GHz) have also been used to estimate sea ice thickness **[8-12]**. These algorithms utilize the dependence of brightness temperature on salinity changes during the ice growth phase **[13]**, and can only be used to measure the thickness of very thin ice (less than 0.2 or 0.3 m) **[8, 12, 14]**. The thickness of thicker sea ice (0.5-1.0 m, depending on ice temperature and salinity) has been estimated using L-band radiometer data (1.4 GHz), such as that from the SMOS (Soil Moisture and Ocean Salinity) mission **[15]**.

Retrieval of lake ice thickness from satellite imagery has received much less attention than for sea ice thickness. A few studies have shown the potential of using passive microwave data to retrieve ice thickness over lakes **[16-18]**. Kang et al. (2010, 2014) studied the sensitivity of the Advanced Microwave Scanning Radiometer-Earth Observing System (AMSR-E) brightness temperature (T_B) to estimate seasonal evolution of ice thickness from Great Slave Lake (GSL) and Great Bear Lake (GBL), Canada, using the 6.9-18.7 GHz frequency channels. Estimated ice thickness derived from 18.7 GHz V-polarization data compared well with coincident in-situ measurements with an average mean bias error (MBE) of 0.06 m and root mean square error (RMSE) of 0.19 m over the period 2002-2009. However, the spatial footprint of the lower frequencies of passive microwave sensors is relatively large (20-50 km) **[19]**, while the higher frequencies are more sensitive to the atmosphere. This limits the use of this data to only the largest lakes of the northern hemisphere, unless the brightness temperatures are corrected for atmospheric effects. Ice thickness can be estimated at a finer spatial resolution (~1 km) using data available from thermal sensors (TIR) **[19-20]**. The estimation is based on satellite-derived ice surface temperature and the ice surface heat balance equation **[21-22]**. Methods proposed to date use an empirical relationship

between snow depth (h_s) and ice thickness (H_i) with the assumption of a linear temperature profile within the snow and ice **[10, 14, 21-22]**. In these methods, assumptions need to be made about ice and snow density as well as on-ice snow depth distribution. Several studies **[9, 12, 23]** have focused on thin (new) ice for which it is reasonable to assume that the ice surface is snow-free. For thicker ice, it has been shown that the retrieval of ice thickness using TIR data is very sensitive to snow depth **[10]**. It is possible to use retrieved snow depth values computed from AMSR-E data over sea ice. However, it has been shown that these retrieved snow depths are biased when the ice is thin **[24]**, which has been the range of interest in previous studies retrieving ice thickness from TIR sensors for sea ice.

In this study, an improvement to the previous approach using TIR data and a surface heat balance equation is proposed. The approach is based on the use of Moderate Resolution Imaging Spectroradiometer Lake Ice Surface Temperature (MODIS LIST) and with snow depth calculated by the 1-D thermodynamic Canadian Lake Ice Model (CLIMo), and is developed and evaluated over GSL and Baker Lake, Canada. Ice thickness is estimated for 12 ice seasons (2002-2014) and the accuracy of retrieved ice thickness is compared with in-situ observations from the Canadian Ice Service. The objectives of this paper are to: 1) improve the accuracy of ice thickness retrievals from MODIS LIST in comparison to previously proposed approaches, by using a diagnostically calculated snow depth (from CLIMo) instead of an empirical relationship; and 2) assess the applicability of the new method to estimate lake ice thickness from MODIS LIST data for ice thickness up to approximately 1.5 m. The accuracy of the retrieval algorithm is applied first on GSL, which is large and deep with thinner ice thickness and then tested over Baker Lake, which has typically thicker ice thickness than GSL. This study contributes to work on thermal imagery-based ice thickness retrieval where snow depth data over lake ice is not available.

II. STUDY AREA

This study was carried out on GSL and Baker Lake, which are both freshwater lakes located in the subarctic continental climate zone of Canada. GSL is the second largest lake of the Mackenzie River Basin, after GBL. The lake is large and deep, with the mean and maximum depth of 41 m and 614 m, respectively, and an area of 27,000 km^2 (Fig. 1) **[25]**. GSL reaches the temperature of maximum density twice in a year, with complete overturn occurring once in the spring and again in the fall **[26]**. The lake is covered by ice usually from December to May with a range of -1.5 to -41.7 °C in air temperature during winters 2002-2014 based on the Yellowknife Airport weather station. For this study, meteorological data used to force CLIMo was obtained from the Yellowknife Airport weather station, (62° 21′ N, 114° 21′ W; 205.7 m a.s.l.) located close to Back Bay on the north shore of GSL (Fig. 1). In-situ observations were available only for the Back Bay site; therefore, a MODIS LIST pixel was retrieved close to this site but far enough away to avoid land contamination. Baker Lake is located 320 km inland from Hudson Bay in the Territory of Nunavut. The lake has an area of 182.2 km^2, with maximum depth of 60 m. Baker Lake is covered by ice usually from November to May with a maximum of -2.3 m ice thickness **[27]**. According to the statistics from Environment and Climate Change Canada for 2002-2014, the monthly average temperature, acquired from the Baker Lake weather station at the north-west of the lake, is below freezing point for most of the time during the year, from October to May. For this study, meteorological data used to force the lake ice model (CLIMo) was obtained from the weather station at 64.32°N, 96.00° W. The location of the MODIS pixels and weather stations used in the present are shown in Fig. 1.

III. DATA AND METHODS

A) MODIS Lake Ice Surface Temperature (LIST)

MODIS UW-L3 Lake Ice Surface Temperature (LIST) products **[22]** generated from MODIS Aqua and Terra Land Surface Temperature and Emissivity (MOD/MYD11_L2, collection 5, 1 km) data available from NASA's Land Processes Distributed Active Archive Center were used in this study. MOD/MYD11_L2 data are produced using the generalized split window approach applied to radiance data products (MOD/MYD021KM) along with geolocation (MOD/MYD03), atmospheric temperature and water profile (MOD07_L2), cloud mask (MOD/MYD35_L2), quarterly land cover (MOD/MYD12Q1), and snow cover (MOD/MYD10_L2) products **[28]**. LIST observations are separated into either a day-time bin (from 6 am to 6 pm) or a night-time bin (from 6 pm to 6 am of the next day), not by solar angle such as the number of hours of daylight and darkness. In this study, only night-time observations were used as to exclude the influence of incident shortwave radiation in the heat balance equation described below (Section II D) **[18, 29]**. MODIS UW-L3 data have previously been evaluated against in-situ observations during the open water season for various lakes, including GSL, and shown to have an average MBE of 1℃ (RMSE=4 ℃) **[30]**. Unfortunately, no in-situ observations are available for MODIS UW-L3 LIST data evaluation during the winter season. However, Kheyrollah Pour et al. (2012) **[25]** compared MODIS LIST data with those obtained from two 1-D numerical lake models, CLIMo and the Freshwater Lake Model (FLake) for GSL. For Back Bay on GSL, the MBE was 1.40℃ and 3.51℃ for CLIMo and FLake, respectively. For this study, 1127 and 1416 MODIS images are used for GSL and Baker Lake, respectively.

B) In-situ ice thickness and snow depth measurements

Lake ice thickness and snow depth measurements from Back Bay (near Yellowknife, NWT) and Baker Lake for the periods 2002-2014 were downloaded from the Canadian Ice Service (CIS) website (https://www.ec.gc.ca/glaces-ice/?lang=En&n=E1B3129D-1) to evaluate the proposed

approach. In this dataset, ice thickness and snow depth are measured approximately once a week, starting shortly after freeze-up when the ice is safe to walk on, until break-up before the ice becomes unsafe. Snow depth measurements are used to estimate the ratio of snow depth on land versus snow depth on the ice. This ratio defines the snow scenario used in the CLIMo runs. Ice thickness measurements are used to obtain the empirical relationship between ice thickness and snow depth for this site and also to evaluate retrieved ice thickness from MODIS.

C) Canadian Lake Ice Model (CLIMo)

CLIMo **[31]**, is an adaptation of the one-dimensional (1-D) thermodynamic sea ice model by Flato and Brown **[32]**. The model was developed to simulate ice phenology, thickness and ice composition on lakes of various depths. In the present study, CLIMo was used to calculate upward and downward longwave radiation, sensible and latent heat fluxes as well as snow depth. CLIMo performs surface energy budget calculations to obtain net flux at the ice, snow or open water surface, solving the heat conduction problem using an implicit-in-time centered-in-space finite difference scheme with the ice/snow slab discretized into an arbitrary number of thickness layers. The 1-D heat conduction equation **[33]** solved by CLIMo is expressed as,

$$\rho C_P \frac{\partial T}{\partial t} = \frac{\partial}{\partial z}(k \frac{\partial T}{\partial z}) + F_{SW} I_0 (1-\alpha) K e^{-Kz} \qquad (1)$$

where $T(z,t)$ is the temperature within the ice or snow, t is time and z is depth measured positive downward from the upper surface, ρ is density, C_P is heat capacity, k is thermal conductivity, F_{SW} is downward shortwave radiation flux, I_0 is fraction of shortwave radiation flux that penetrates the surface, α is surface albedo, and K is the bulk extinction coefficient for penetration of shortwave radiation.

The heat conduction equation is subject to two boundary conditions. First, the ice underside is always at the freezing point of water,

$$T(h,t) = T_f \qquad (2)$$

where thickness, h, is considered as the total thickness of ice and snow. Second, the upper surface is either at the melting temperature, or the heat flux at the surface is equal to the conductive flux through the ice. These conditions can be expressed as

$$T(0,t) = T_m \qquad F_0 > 0, \hat{T}(0) \geq T_m$$

$$k \frac{\partial T}{\partial z}|_{z=0} = F_0 \qquad \text{otherwise} \qquad (3)$$

where T_m is the melting temperature at the surface, F_0 is the net heat flux absorbed at the surface and $\hat{T}$ is the estimated surface temperature prior to solving the heat conduction equation (Eq. 1). When melt occurs at the upper surface, the temperature is fixed at the melting point of fresh water (either snow or relatively fresh ice). A detailed description of CLIMo can be found in **[31]**.

1) CLIMo Parameterization: The parameterization scheme used in CLIMo follows closely that of Ebert and Curry **[29]**. CLIMo calculates ice thickness and snow depth from mass and density of snow and ice, as well as using information from forcing (meteorological) data. The layer thickness of snow and ice is used to parameterize snow conductivity and heat capacity, which are defined as

$$k(z) = c_1 \rho_s^2 + c_2 2^{[T(z)-c_3]c_4} \qquad z < h_s \qquad (4)$$

$$\rho C_P(z) = \rho_s [c_5 + c_6 T(z)] \qquad z < h_s \qquad (5)$$

where z is depth measured from the upper surface and h_s is the snow depth, and $c_1 = 2.845 \times 10^{-6}$ *W m^5 K^{-1} kg^{-2}*, $c_2 = 2.7 \times 10^{-4}$ *W m^{-1} K^{-1}*, $c_3 = 233$ *K*, $c_4 = 1/5$ *K^{-1}*, $c_5 = 92.88$ *J kg^{-1} K^{-1}*, *and* $c_6 = 7.364$ *J kg^{-1} K.* The values used for conductivity (k_{if}) and heat capacity ($\rho_i C_{Pi}$) of freshwater ice in CLIMo are, $k_{if} = 2.034$ Wm^{-1} K^{-1} and $\rho_i C_{Pi} = 1.883 \times 10^{-6}$ Jm^{-3} K^{-1}. The melting ice parameterization is based on Arctic lake-ice observations from Heron and Woo **[36]** and the cold ice albedo is from Maykut **[31]**.

Forcing data: CLIMo was forced with daily averages of 2-m air temperature, relative humidity, cloud cover, wind speed and snow accumulation from the Yellowknife weather station (for GSL) and from the Baker Lake weather station (for Baker Lake). The simulation was carried out using a time step of 1 day and run over the entire study period (2002-2014). The initial state was specified by including an additional year of forcing data (year 2001) in order to avoid an effect of the spin-up phase of the model run on the period of investigation. Measured snow accumulation was from the weather station on the Yellowknife close to the Back Bay lake site. As snow accumulation on land can be different from that on a lake, notably due to wind effects, CLIMo can be run with different snow accumulation scenarios **[31, 37-38]**. The scenarios account for wind redistribution of snow on the open ice surface (from 0% to 100% on the ice surface of the amount measured at the station on land). Fig. 2 shows the percentage of snow accumulation on ice in Back Bay calculated from in-situ snow depth on ice and weather station snow depth measurements for the study period (2002-2014). Snow depth over land (from the weather station) and over the lake ice surface (from in-situ measurements) are averaged for each year separately. The average percentage of snow depth on lake ice is calculated first for each year, and then the yearly means are averaged for the entire study period. As is shown in Fig. 2, the average value of the percentage of snow on the lake ice surface relative to that measured at the

weather station is 70%. Therefore, CLIMo was run with a 70% snow scenario for the whole study period.

D) Ice Thickness Calculation using MODIS LIST

Ice thickness is estimated from MODIS LIST pixel data by solving a heat balance equation **[14, 21]**. For this study, only night-time MODIS LIST data were used to exclude the influence of incident shortwave radiation in the heat balance, which is one of the main sources of uncertainty in the algorithm **[20] [27]**. The equation for heat balance at the upper surface of the lake during night-time is

$$F_l^{up} + F_l^{dn} + F_s + F_e + F_C = 0 \quad (6)$$

where F_l^{up} is the upward longwave radiation, F_l^{dn} is the downward longwave radiation, F_s is the sensible heat flux, F_e is latent flux, and F_C is the conductive heat flux. In solving Eq. 6, the fluxes of longwave radiation, sensible and latent heat are given either by parameterization or by a separate model (in this case the parameterizations are included in CLIMo). This enables Eq. 6 to be solved for the conductive flux, from which the ice thickness can be retrieved. The conductive flux is estimated by assuming a linear temperature profile in the snow and ice

$$F_C = \gamma(T_f - T_s) \quad (7)$$

where $\gamma = (k_i k_s)/(k_s H_i + k_i h_s)$ is the thermal conductance of the ice-snow slab, T_f is the freezing temperature of freshwater (273.15 K), T_s is the MODIS LIST for the specified pixel, H_i and h_s are ice thickness and snow depth, respectively. The conductivity of ice (k_i) is determined using

$$k_i = k_0 + \beta S_i/(T_s - T_f) \quad (8)$$

where $k_0 = 2.22(1 - 0.00159 \times T_s)$, which is the conductivity of pure ice, meaning ice with no bubbles or air pockets, β is 0.13 Wm^{-1}, and S_i is the lake ice salinity in parts per thousand (ppt) and T_S is the ice temperature from MODIS. The thermal conductivity of natural ice is influenced by air bubbles and inclusions of unfrozen water containing dissolved impurities **[39]**. Schwerdtfeger derived a theoretical relationship between the fraction air-bubble content and the thermal conductivity of pure ice **[40]**. Here, the conductivity equation was adapted to $k_0 = 1.95(1 - 0.00159 \times T_s)$. Moreover, GSL is a freshwater lake, hence S_i is assumed to be 1.0 ppt. The conductivity of snow (k_s) was determined using $k_s = 2.845 \times 10^{-6}\rho_{snow}^2 + 2.7 \times 10^{-4}(2^{(T_s-233)/5})$ **[39]**. The MODIS surface temperature was used for T_s and an average snow density (ρ_{snow}) of 330 kg m^{-3} was used in the model runs. The density of on-ice snow has been found to be 120% higher than on-land snow nearby **[41-42],** hence the density was adjusted accordingly, as has been done in previous studies **[43]**. Finally, the ice thickness is retrieved using Eq. 7 and the thermal conductance, from which the following expression is obtained

$$H_i = \frac{k_i \times k_s - (\frac{F_C}{T_S - T_f} \times k_i \times h_s)}{\frac{F_C}{T_S - T_f} \times k_s} \quad (9)$$

To evaluate the impact of snow depth on the retrieval of ice thickness from MODIS, experiments were carried out using two different approaches. In the first approach, an empirical relationship between snow depth and ice thickness similar to that proposed by Doronin **[44]** was used. Due to difficulties in obtaining accurate snow depth measurements on ice from spaceborne sensors, the empirical relationship is frequently employed **[10, 14, 20-21]**. In the second approach, the snow depth calculated by CLIMo was used. In both experiments, all fluxes at the upper surface of the ice or snow from Eq. 6 were calculated from CLIMo, except for the conductive flux (Eq. 7) which was calculated differently for the two approaches due to their respective way of considering snow depth.

For this study, coincident in-situ measurements of snow depth and ice thickness from Back Bay (2002-2014) were used to derive the empirical relationship between h_s and H_i. No ice thickness measurements were available for ice thinner than 0.2 m, hence, in the first experiment, the approach followed that of Doronin **[44]** for ice thinner than 0.2 m. For ice thicker than 0.2 m, the given in-situ data can be used, yielding the following relationships between snow depth, h_s, and ice thickness H_i

$$\begin{aligned} h_s &= 0 && for\ H_i < 0.05\ m \\ h_s &= 0.05H_i && for\ 0.05\ m \le H_i \le 0.2\ m \\ h_s &= 0.2H_i && for\ H_i > 0.2\ m \end{aligned} \quad (10)$$

Note that this is the same as that from Doronin **[44]** except when ice thickness is greater than 0.2 m, where h_S=0.1Hi.

IV. EXPERIMENTAL SETUP

Two experiments were carried out to investigate the treatment of snow depth on ice thickness retrieved with MODIS LIST. In the first experiment, the snow depth parameterization (Eq. 10) was used, while in the second experiment, snow depth from CLIMo (70% snow scenario) was used. For both experiments the heat fluxes were calculated using CLIMo, and the same MODIS LIST were used, hence the only difference is the treatment of snow depth.

A third experiment was carried out to assess the retrieval of ice thickness on Baker Lake using the proposed approach (snow depth from CLIMo). The same snow scenario was used for Baker Lake as for GSL.

To assess the ice thickness retrieval outputs, three statistical indices were calculated, the root mean square error

(RMSE), the mean bias error (MBE), and the index of agreement (I_a). The MBE is calculated as the mean of predicted values minus the in-situ observations to show an overestimation (underestimation) of the parameter of interest. RMSE is a comprehensive metric that combines the mean and variance of model errors into a single statistic. I_a is a descriptive measure of model performance. It is dimensionless and bounded by 0 (worst performance) and 1.0 (the best possible performance) **[45]**. The statistics presented herein are calculated for all years of the study (2002-2014).

For all experiments, the ice thickness was calculated from MODIS LIST each day with clear-sky conditions from mid-November until the end of March (2002-2014) using Eq. 9. The period of November to the end of March is selected to avoid the melt season. Determination of ice thickness during the melt season can be problematic using a heat flux approach due to the presence of water on the top of the ice, indicating that there should be no net heat conduction through the ice. While the surface may refreeze, it is still difficult to obtain the signal of conductivity. The melt season begins usually around mid-April, therefore April was not considered in the analysis.

V. RESULTS

A. Assessment of ice thickness from MODIS using the empirical relationship between snow depth and ice thickness for GSL

The estimated ice thickness from MODIS LIST using the empirical snow depth (Eq. 10) for the selected pixel location is in the range of 0.04-1.08 m with an underestimation of ice thickness. The statistics of the differences between the ice thickness from MODIS LIST and in-situ data over the study period are MBE=-0.42 m, RMSE= 0.58 m, and I_a=0.34. The scatterplot of estimated MODIS ice thickness against in-situ measurements is shown in Fig. 3. It can be seen there is a great deal of scatter, especially for ice of thickness greater than 0.4 m.

The scatter and lack of trend could be attributed to various factors, such as inaccuracies in the calculated longwave, sensible or latent heat fluxes, the parameterizations used in the conductive heat flux, or unmasked clouds in the MODIS LIST. The next section will show that it is likely the empirical relationship between snow depth and ice thickness that is leading to the poor estimates of ice thickness.

B. Assessment of the ice thickness from MODIS using CLIMo parameterization for GSL

Ice thickness was then calculated from MODIS LIST with the snow depth calculated from CLIMo. The only difference between this section and the previous section is the snow depth used in the conductive heat flux. The estimated ice thickness from MODIS for the selected location was in the range of 0.01-1.2m over the full duration of the ice season.

The scatterplots and statistics of MODIS ice thicknesses in comparison with in-situ ice thickness measurements are shown in Fig. 4. The statistics improved significantly in comparison to the previous approach (MBE = 0.07 m, RMSE =0.17 m, and I_a=0.9). The improvement of standard deviation and standard error from using the snow depth from CLIMo as compared with the empirical method are 0.32 to 0.15 and 0.03 to 0.01, respectively. Ice thickness calculated from MODIS LIST with the snow depth calculated from CLIMo shows a correlation of 0.85 (Pearson correlation) with in-situ observations for GSL, whereas the empirical method shows a correlation of 0.06.

The time series of estimated MODIS ice thickness as well as simulated snow depth in comparison to in-situ observations are shown in Fig. 5 (ice thickness values are shown in negative to indicate distance from the snow/ice interface). It can be seen that there are variations in ice thickness for different years between these datasets. For example, MODIS indicates relatively thicker ice than in-situ measurements for years 2006-2009 and 2011 for GSL. However, estimated ice thicknesses agree well in general with in-situ measurements. Some of the differences are likely due to snow depth variability between years as shown in Fig. 2, knowing that an average value of 70% for the snow scenario was applied to all years for all CLIMo runs. The snow density was also assumed to be 330 kg m^{-3} during all winter seasons, which is an approximation. The density of snow can vary within a winter season as well as between different years. Moreover, differences may be due to the different observational scales, as MODIS observations cover an area of 1 km x 1 km, whereas the in-situ ice thickness observations are collected at a drill hole of a few cm. It is important to keep in mind that errors are unavoidable and data might have a finite uncertainty when using in-situ data as a reference dataset.

C. *Assessment of the ice thickness from MODIS using CLIMo parameterization for Baker Lake*

The proposed approach was also tested on Baker Lake for the 2002-2014 period. The method was applied in the same manner as for GSL, with forcing data from the Baker Lake weather station and MODIS LIST from a pixel over the lake. The statistics in comparison to in-situ measurements are: MBE = 0.45 m, RMSE =0.73 m, and I_a = 0.7. While the agreement is not quite as good as it is for GSL, it should be noted that the ice is on average thicker on Baker Lake (0.01-2m over the full duration of the ice season), and the ice thickness retrieval described in Section III D was not work as well for thick ice as for thin ice due to the assumption of a linear temperature profile in the ice and snow layers. The results show that this approach is limited to ice thickness estimations of less than 1.7 m.

D. Assessment of snow and ice thickness over an ice season

Snow cover plays a crucial role in controlling ice thickness, it is therefore important to monitor variations in snow depth to be able to interpret the ice growth. Evaluation of ice thickness is especially sensitive to the timing and amount of

snow accumulation in the early as well as late seasons. Fig. 6 shows a visual comparison of in-situ and calculated snow depth and ice thickness values during two single winter seasons (2004-2005 for GSL and 2005-2006 for Baker Lake). As all years follow similar trends, these two winters are selected arbitrarily. The simulated snow depth obtained with CLIMo agrees well with in-situ measurements collected from Canadian Ice Service for GSL (MBE = 0.07 m, RMSE =0.17 m, I_a = 0.8) and for Baker Lake (MBE = 0.45 m, RMSE =0.73 m, I_a = 0.7). Maximum ice thickness retrieved by MODIS for GSL is -1.23 m on 23 March 2005 when snow was 0.34 m deep, whereas ice thickness measured in-situ reached its maximum of 1.18 m at the end of March 2007. For Baker Lake the maximum accurate ice thickness was on 3 April 2006 of 1.7 m. The algorithm is not accurate when the ice thickness is greater than 1.7 m; therefore the statistics is re-calculated for the ice thickness less than 1.7 m, which improved the results by MBE = 0.1 m, RMSE =0.3 m, I_a = 0.8.

E. Sensitivity Study

In the previous sections is was shown that the ice thickness from MODIS LIST is in better agreement with in-situ measurements when snow thickness from CLIMo is used, as compared to when snow thickness is parameterized as a function of ice thickness. The heat flux used for the calculation of ice thickness was the same for both cases, with the only difference between the two being the snow depth. Hence, it can be concluded that the improved agreement is due to the snow thickness.

However, the sensitivity of the ice thickness retrieval to the heat flux has not yet been discussed, or compared with the sensitivity to snow depth. Previous studies have shown that for conditions characteristic of sea ice in the Arctic, the ice thickness is more sensitive to snow depth than any of the other input data for a nighttime retrieval, with a change in ice thickness of 66% of its mean value when the snow depth is varied by +/- 10 cm **[10]**. This is more than the sensitivity to heat flux input data, found to be 27%-41% of the mean ice thickness in a separate study **[21]**. To investigate the sensitivity of the ice thickness to both the snow depth and the heat fluxes for conditions relevant to the lakes investigated here, a sensitivity study was carried out for GSL for the months of December 2005 and February 2006. However, because the results for each of the two months were similar, only those from February 2006 are shown.

First, the equations for sensible, latent and radiative heat fluxes solved by CLIMo were examined in tandem with **[10]** to determine which of the input variables should be perturbed to obtain a representative distribution of heat fluxes. Considering the inputs of air temperature, relative humidity, cloud cover, wind speed and snow accumulation, it was decided to perturb the air temperature and windspeed. The study by Wang et al. **[10]** found the ice thickness was not very sensitive to the relative humidity. Snow accumulation would impact the snow thickness calculated by CLIMo, but would have a smaller impact on the radiative, sensible and latent heat fluxes, and cloud cover was not considered since clear sky images were chosen for the present study. It was then necessary to define typical distributions of the errors of the wind speed and air temperatures from which samples could be drawn to generate distributions of the heat fluxes. As we do not have in-situ measurements that are independent from the weather station data, we chose to define the error as the difference between the weather station measurement and re-analysis data (ECMWF ERA-Interim). Note that the ECMWF data consist of a single daily output on grid of 0.125 degree resolution. To compare with the station data, the station data were averaged for each day, and the ECMWF data from the grid point closest to the station location was used. From these distributions, standard deviations of the errors air temperature and wind (δTair and δW) were defined. A specified number of samples (n=500) was then chosen from a Gaussian distribution with mean values given by the station data averaged over February 2006 and standard deviations δTair and δW. These samples were used to run CLIMo n times. From these CLIMo runs, a mean value and standard deviation for each term in the heat balance equation was obtained, in addition to the mean and standard deviation of the conductive heat flux ($\overline{Fc}$ and δFc), and of the CLIMo snow depth ($\overline{Hs}$ and δHs) (Table 1).

Using these results, three different experiments were carried out (Table 2). The first experiment was carried out to investigate the sensitivity of the retrieved ice thickness to variations in the conductive heat flux. In this experiment, the snow depth was held constant at $\overline{Hs}$, while Fc was varied by choosing 500 samples from a distribution $N(\overline{Fc},\delta Fc)$. In the second experiment, Fc was held constant at $\overline{Fc}$ while the snow depth was varied by choosing 500 samples from the distribution $N(\overline{Hs},\delta Hs)$. For the third experiment, Fc was varied by choosing 500 samples from a distribution $N(\overline{Fc},\delta Fc)$ and the snow depth was parameterized as a function of the ice thickness. In all cases the MODIS temperature was fixed at the average value for February 2006 of 251.8 K and the ice thickness was retrieved using Eq. (7) and (9). The results, are given in Table 2. Comparing the standard deviation of ice thickness (δHi) for EXP1 and EXP2 demonstrates that the change in ice thickness was more significant when the snow depth was varied, as compared to the conductive heat flux, consistent with previous studies. Comparing δHi for EXP1 and EXP3 it can be seen that δHi is larger when the snow depth parameterization is used, and the mean value is farther from the in-situ mean value for February 2006 (Fig. 7).

IV. CONCLUSION

This paper dealt with estimation of ice thicknesses from MODIS LIST using two different methods of incorporating snow depth information in the ice thickness retrieval. In the first method, an empirical relationship between snow depth and ice thickness was used, while in the second method,

snow depth was calculated by CLIMo. Both methods used heat fluxes calculated from CLIMo, except for the conductive flux, which was calculated independently. The results showed an improvement of ice thickness estimation, reducing the MBE by 0.35 m in magnitude, when using snow thickness from CLIMo in comparison to the approach using an empirical relationship between snow depth and ice thickness. The latter approach has been applied in several previous studies **[10, 14, 20-22].** These studies report errors that increase with increasing ice thickness **[14, 20-22]**, with the snow parameterization a likely source of error **[10, 21]**, in addition to errors from input data (e.g. wind speed, air temperature) and heat flux parameterizations **[22]**. The present study demonstrates that when accurate snow depth information is available, ice of thickness up to 1.7 m can be retrieved. In order to minimize the uncertainties associated with the forcing data, calculations were carried out using forcing data from a nearby weather station.

Further evaluations of the retrieval algorithm are planned over the entire area of GSL and Baker Lake as well as the Laurentian Great Lakes. For these studies, data from re-analysis or a numerical weather forecasting model will be used to force CLIMo for every pixel over the lakes.

Due to the spatial resolution of 1-km, the ice thickness from MODIS may be more useful in comparison to passive microwave data in regions where relatively high spatial resolution is required. The main limitations of using LIST from MODIS to determine ice thickness is that the number of clear-sky pixels may be limited, and it can be difficult to determine the accuracy of the cloud mask, in particular for night-time conditions **[46]**. However, it should be noted that in order for the retrieved ice thickness to be useful for operational forecasting (e.g. combining the ice thickness observations with a model state using data assimilation) it is not necessary to have ice thickness observations available at each point in the spatial domain on a daily basis. In addition, the development of quality control measures to eliminate gross errors (such as unmasked clouds), as well as methods to estimate the uncertainty in the observations, are both requirements before the observations can be used in an operational context.

ACKNOWLEDGMENT

This work was supported by a Marine Environmental Observation Prediction and Response Network (MEOPAR) grant to K. A. Scott.

REFERENCES

[1] V. I. Lytle and S. L. Ackley, "Heat flux through sea ice in the western Weddell Sea: Convective and conductive transfer processes," *J. Geophys. Res.*, vol. 101(C4), pp. 8853-8868, 1996.

[2] M., Sturm, D. K. Perovich, and J. Holmgren, "Thermal conductivity and heat transfer through the snow on the ice of the Beaufort Sea," *J. Geophys. Res.*, vol. 107(C21), pp. 8043, 2002.

[3] S. Laxon, N. Peacock, and D. Smith, "High interannual variability in sea ice thickness in the Arctic region," *Nature*, vol. 425(6961), pp. 947–950, 2003.

[4] R. Kwok and G.F. Cunningham "ICESat over Arctic sea ice: estimation of snow depth and ice thickness," *J. Geophys. Res.*, vol. 113(C8), C08010 (doi: 10.1029/2008JC004753), 2008.

[5] S. Martin, R. Drucker, R. Kwok, and B. Holt, "Estimation of the thin ice thickness and heat flux for the Chukchi Sea Alaskan coast polynya from Special Sensor Microwave/Imager data, 1990–2001," *J. Geophys. Res.*, vol. 109(C10), pp. 10012, 2004.

[6] Y. N. T. Kurtz, N. Galin, M. Studinger, "An improved CryoSat-2 sea ice freeboard retrieval algorithm through the use of waveform fitting", *The Cryosphere*, vol. 8, pp. 1217–1237, 2014.

[7] R. Ricker, S. Hendricks, V. Helm, H. Skourup, M. Davidson, "Sensitivity of CryoSat-2 Arctic sea-ice freeboard and thickness on radar-waveform interpretation", The Cryosphere, vol. 8, pp. 1607–1622, 2014.

[8] R. Kwok, G. F. Cunningham, "Variability of Arctic sea ice thickness and volume from cryostat-2", *The Royal Soci.*, pp. 1471-2962, 2014, DOI: 10.1098/rsta.2014.0157.

[9] S. Nihashi, K. Ohshima, T. Tamura, Y. Fukamachi, and S. Saitoh, "Thickness and production of sea ice in the Okhotsk Sea coastal polynyas from AMSR-E," *J. Geophys. Res.*, vol. 114, no. C10, pp. C10025-1–C10025-15, Oct. 2009.

[10] X. Wang, J. Key, and Y. Liu, "A thermodynamic model for estimating sea and lake ice thickness with optical satellite data," *J. Geophys. Res.*, vol. 115, no. C12, pp. C12035-1–C12035, Dec. 2010.

[11] R. K. Singh, S. R. Oza, N. K. Vyas, and A. Sarkar, "Estimation of thin ice thickness from the advanced microwave scanning radiometer- EOS for coastal polynyas in the Chukchi and Beaufort seas," *IEEE Trans. Geosci. Remote Sen.*, vol. 49(8), pp. 2993–2998, 2011.

[12] T. Tamura, and K. I. Ohshima, "Mapping of sea ice production in the Arctic coastal polynyas," *J. Geophys. Res.*, vol. 116(C7), pp. C07030, 2011.

[13] K. Naoki, J. Ukita, F. Nishio, M. Nakayama, J.C. Comiso, A. Gasiewski, "Thin sea ice thickness as inferred from passive microwave and in-situ observations," *J. Geophys. Res.*, vol. 113, pp. C2, doi.10.1029/2007JC004270,2008.

[14] K. A. Scott, M. Buehner, and T. Carrieres, "An assessment of sea-ice thickness along the Labrador coast from AMSR-E and MODIS data for operational data assimilation," *IEEE Trans. Geosci. Remote Sens.*, vol. 25, no. 5, pp. 2726-2737, 2014.

[15] X. Tian-Kunze, L. Kaleschke, N. Maaß M Makynen, N. Serra, M. Drusch and T.Krumpen, "SMOS-derived thin sea ice thickness: algorithm baseline, product specifications and initial verification," *The Cryo.*, vol. 8, pp. 997-1018, 2014.

[16] D. K. Hall, J. L. Foster, A. T. C. Chang, and A. Rango, "Freshwater ice thickness observations using passive microwave sensors," *IEEE Trans. Geosci. Remote Sens.*, vol. GRS-19, no. 4, pp. 189–193, 1981.

[17] D. K. Hall, "Active and passive microwave remote sensing of frozen lakes for regional climate studies," *Proc. Snow Watch—Detection Strategies Snow Ice, Glaciological Data Rep GD-25.*, pp. 80–85, 1993.

[18] K.-K. Kang, C. R. Duguay, S. E. L. Howell, C. P. Derksen, and R. E. J. Kelly, "Sensitivity of AMSR-E brightness temperature to the seasonal evolution of lake ice thickness," *IEEE Geosci. Remote Sens. Let.*, vol. 7, no. 4, pp. 751-755, 2010.

[19] K.-K. Kang, C. R. Duguay, J. Lemmetyinen, and Y. Gel, "Estimation of ice thickness on large northern lakes from AMSR-E brightness temperature measurements," *Remote Sens. Env.*, vol. 150, pp. 1-19, 2014.

[20] Y. Yu and R. Lindsay, "Comparison of thin ice thickness distributions derived from RADARSAT Geophysical Processor System and advanced very high resolution radiometer data sets," *J. Geophys. Res.*, vol. 108, no. C12, pp. 3387–3397, Dec. 2003.

[21] Y. Yu, and D. Rothrock, "Thin ice thickness from satellite thermal imagery," IEEE *Trans. Geosci. Remote Sens.*, vol. 25, no. 5, pp. 2726-2737, Nov. 1996.

[22] M. Mäkynen, B. Cheng, and M. Similä, "On the accuracy of thin-ice thickness retrieval using MODIS thermal imagery over Arctic first-year ice," *Annals of Glacio.*, vol. 54(62), pp. 87-96, 2013.

[23] A. Preußer, S. Willmes, G. Heinemann, and S. Paul, "Thin-ice dynamics and ice production in the Storfjorden polynya for winter seasons 2002/2003-2013/2014 using MODIS infrared imagery," *The Cryos.*, vol. 9, pp. 1063-1073, May. 2015.

[24] D. Cavalieri, T. Markus, A. Ivanoff, J. Miller, M. Brucker, J. Maslanik, J. Heinrichs, A. Gasiewski, C. Leuschen, W. Krabill, and J. Sonntag, "A comparison of snow depth on sea ice retrievals using airborne altimeters and an AMSR-E simulator," *IEEE Trans. Geosci. Remote Sens.*, vol. 50, no. 8, pp. 3027–3040, Aug. 2012.

[25] H. Kheyrollah Pour, C. R. Duguay, A. Martynov, and L. C. Brown, "Simulation of surface temperature and ice cover of large northern lakes with 1-D models: a comparison with MODIS satellite data and in situ measurements," *Tellus A*, vol. 64, pp. 17614, Feb. 2012.

[26] W. R., Rouse, P. D. Blanken, C. R. Duguay, C. J. Oswald and W. M. Schertzer, "Climate-Lake Interactions," in *Cold Region Atmospheric and Hydrologic Studies: The Mackenzie GEWEX Experience Volume 2*: *Hydrologic Processes*, M. K. Woo, Ed., Berlin, Germany, Springer-Verlag, 2008, Ch. 8, pp. 139–160.

[27] A. S. Medeiros, C. E. Friel, S. A. Finkelstein, R. Quinlan, "A high resolution multi-proxy record of pronounced recent environmental change at Baker Lake," *Nunavut J. of Paleolim.*, vol. 47, no. 4, pp. 661-676, 2012.

[28] Z. Wang, "Collection-5 MODIS Land Surface Temperature Products Users' Guide. ICESS, *University of California, Santa Barbara*.

[29] S. Adams, S. Willmes, D. Schröder, G. Heinemann, M. Bauer, and T. Krumpen, "Improvement and sensitivity analysis of thermal thin-ice thickness retrieval," *IEEE Trans. Geosci. Remote Sens.*, vol. 51, no. 6, pp. 3306-3318, June. 2013.

[30] H. K. Kheyrollah Pour, C. R. Duguay, R. Solberg, and Ø. Rudjord, "Impact of satellite-based lake surface observations on the initial state of HIRLAM. Part I: evaluation of remotely-sensed lake surface water temperature observations," *Tellus A*, vol. 66, pp. 21534, May. 2014.

[31] C. R. Duguay, G. M. Flato, M. O. Jeffries, P. Ménard, K. Morris, and W. R. Rouse, "Ice-cover variability on shallow lakes at high latitudes: model simulations and observations," *Hydrol. Process*, vol. 17, pp. 3465-3483, 2003.

[32] G. M. Flato, and R. D. Brown, "Variability and climate sensitivity of landfast Arctic sea ice," *J. Geophys. Res.*, vol. 101(C10), pp. 25767-25777, 1996.

[33] G. A. Maykut, and N. Untersteiner, "Some results from a time-dependent thermodynamic model of sea ice," *J. Geophys. Res.*, vol. 76, pp. 1550–1575, 1971.

[34] E. E. Ebert, and J. A. Curry, "An intermediate one-dimensional thermodynamic sea ice model for investigating ice–atmosphere interactions," *J. Geophys. Res.*, vol. 98, pp. 10085–10109, 1993.

[35] R. Heron, and M-K. Woo, "Decay of a high arctic lake-ice cover: observations and modelling," *J. Geophys. Glacio.*, vol. 40, pp. 283-292, 1994.

[36] G.A. Maykut, "Large-scale heat exchange and ice production in the central Arctic," *J. Geophys. Res.*, vol. 87, pp. 7971-7984, 1982.

[37] P. Ménard, R. C. Duguay, G. M. Flato, and W. R. Rouse, "Simulation of ice phenology on Great Slave Lake, Northwest Territories, Canada," *Hydrol. Process*, vol. 16, pp. 3691–3706, 2002.

[38] L.C. Brown, and R. C. Duguay, "A comparison of simulated and measured lake ice thickness using a Shallow Water Ice Profiler," *Hydrol. Process*, vol. 25(19), pp. 2932–2941, 2011.

[39] J. A. Curry, and P. J. Webster, *Thermodynamics of atmospheres and Oceans*. International Geophysics series: Academic press, Ch 2, pp. 276-279, 1999.

[40] P. Schwerdtfeger, "The thermal properties of sea ice," *J. Glacio*, vol. 4, no. 36, pp. 789-807, 1963.

[41] "MSC: Canadian Snow Data CD-ROM, CRYSYS Project, Climate Processes and Earth Observation Division, Meteorological Service of Canada." Downsview, Ontario, Canada, January 2000.

[42] M. Sturm, and G.E. Liston, "The snow coveron lakes of the Arctic Coastal Plain of Alaska, U.S.A.," *J. Glacio*, vol. 49, no. 166, pp. 370-380, 2003.

[43] L.C. Brown, and R. C. Duguay, "Modelling Lake Ice Phenology with an Examination of Satellite-Detected Subgrid Cell Variability," *Adv. Meteo.*, vol. 2012, pp. 19, 2012.

[44] Y. P. Doronin, "Thermal Interaction of the Atmosphere and the Hydrosphere in the Arctic," *Isr. Program for Sci. Transl., Jerusalem*, vol. 85, 1971.

[45] C. J. Wilmott, "On the validation of models", *Phys. Geogr.*, vol. 2, pp. 184–194, 1981.

[46] Y. Liu, J. R. Key, R. A. Frey, S. A. Ackerman, W. P. Menzel, "Nighttime polar cloud detection with MODIS", *Remote Sens of Env.*, vol. 92, pp. 181–194, 2004.

Table captions

Table 1. Standard deviation of heat fluxes, snow thickness and mean snow thickness for 500 CLIMo runs with perturbations drawn from distributions $N(\overline{T}\text{air},\delta\text{Tair})$ and $N(\overline{W},\delta\text{W})$.

Table 2. Experiments carried out to investigate the sensitivity of the ice thickness to the treatment of snow depth and to the conductive heat flux.

Figure captions

Fig.1. Maps showing the location of Great Slave Lake (GSL), and MODIS pixel location, as well as the meteorological weather station of Yellowknife, Northwest Territories, Canada, near Back Bay on GSL.

Fig.2. Percentage of snow depth measured on ice in Back Bay, Great Slave Lake, relative to snow depth measured on the ground at the Yellowknife weather station (2002-2014). Dots represent average percentage of snow depth on lake for each year and bars are standard deviation.

Fig. 3. Scatterplot of estimated ice thickness from MODIS using empirical relationship between snow depths (h_s) and ice thickness (H_i) versus in-situ ice thickness measurements, Back Bay, Great Slave Lake. The units of MBE and RMSE are m. Orange solid line is the correlation fit and the black line is the 1:1 line.

Fig. 4. Scatterplot of estimated ice thickness from MODIS with CLIMo parameterization versus in-situ ice thickness measurements, Back Bay, Great Slave Lake. The units of MBE and RMSE are m. Orange solid line is the correlation fit and the black line is the 1:1 line.

Fig. 5. Time series of estimated ice thickness from MODIS (black dots) and simulated snow depth from CLIMo model (black ×) in comparison with the in-situ measurements from CID (blue), Back Bay, Great Slave Lake.

Fig. 6. Comparison of in-situ and calculated snow depth (CLIMo) and ice thickness (MODIS) for winter seasons 2004-2005 on Back Bay, Great Slave Lake, NWT (upper panel) and 2005-2006 (lower panel), for Baker Lake, Nunavut.

Fig. 7. Histogram comparing the distribution of ice thickness using CLIMo snow depth and simple snow parameterization in comparison with mean in-situ ice thickness for February 2006.

Table 1. Standard deviation of sensible, latent and conductive heat fluxes, snow thickness and mean snow thickness for 500 CLIMo runs with perturbations drawn from distributions $N(\overline{T}\text{air},\delta\text{Tair})$ and $N(\overline{W},\delta\text{W})$

February 2006		***δFs* (W/m²)**	***δFl* (W/m²)**	***δFc* (W/m²)**	$\overline{Hs}$ **(m)**	***δHs* (m)**
$\overline{T}_{\text{air}}$ (°C) = -17.5	δT_{air} = 7.1	16.63	4.21	1.65	0.21	0.07
$\overline{W}$(m/s) = 13.1	δW= 7.1	13.7	3.87	1.64	0.19	0.06

Table 2. Experiments carried out to investigate the sensitivity of the ice thickness to the treatment of snow depth and to the conductive heat flux.

February 2006	$\overline{LIST}$**(K)**	$\overline{Hs}$**(m)**	***δHs* (m)**	$\overline{Fc}$ **(W/m²)**	***δFc* (W/m²)**	$\overline{Hi}$ **(m)**	***δHi* (m)**	***δHi*/$\overline{Hi}$**
EXP1	251.8	0.21	--	9.94	1.65	0.7	0.07	0.05
EXP2	251.8	0.21	0.07	9.94	--	0.9	0.1	0.12
EXP3	251.8	--	--	9.94	1.65	1.02	0.18	0.17

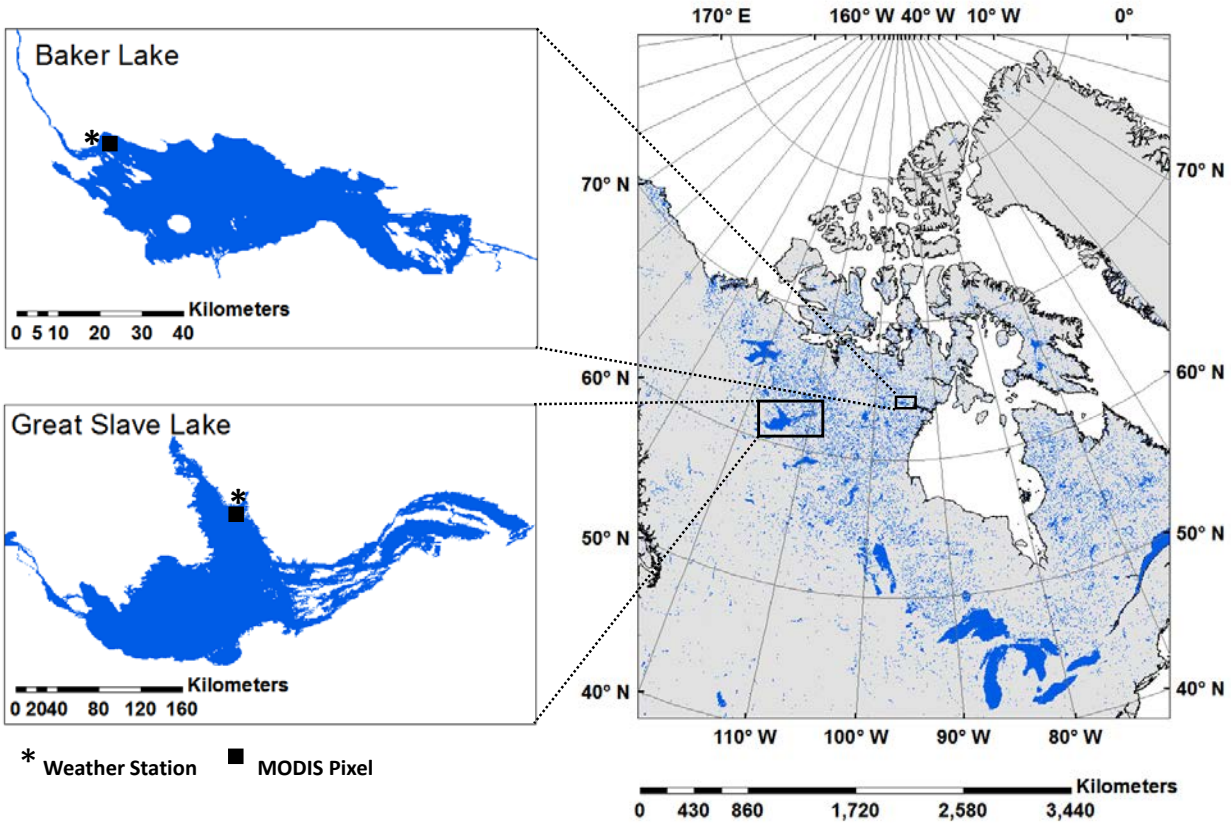
Baker Lake
Kilometers
0 5 10 20 30 40
Great Slave Lake
Kilometers
0 2040 80 120 160
* Weather Station
MODIS Pixel
170° E
160° W
40° W
10° W
0°
70° N
60° N
50° N
40° N
110° W
100° W
90° W
80° W
Kilometers
0 430 860 1,720 2,580 3,440

Fig.1

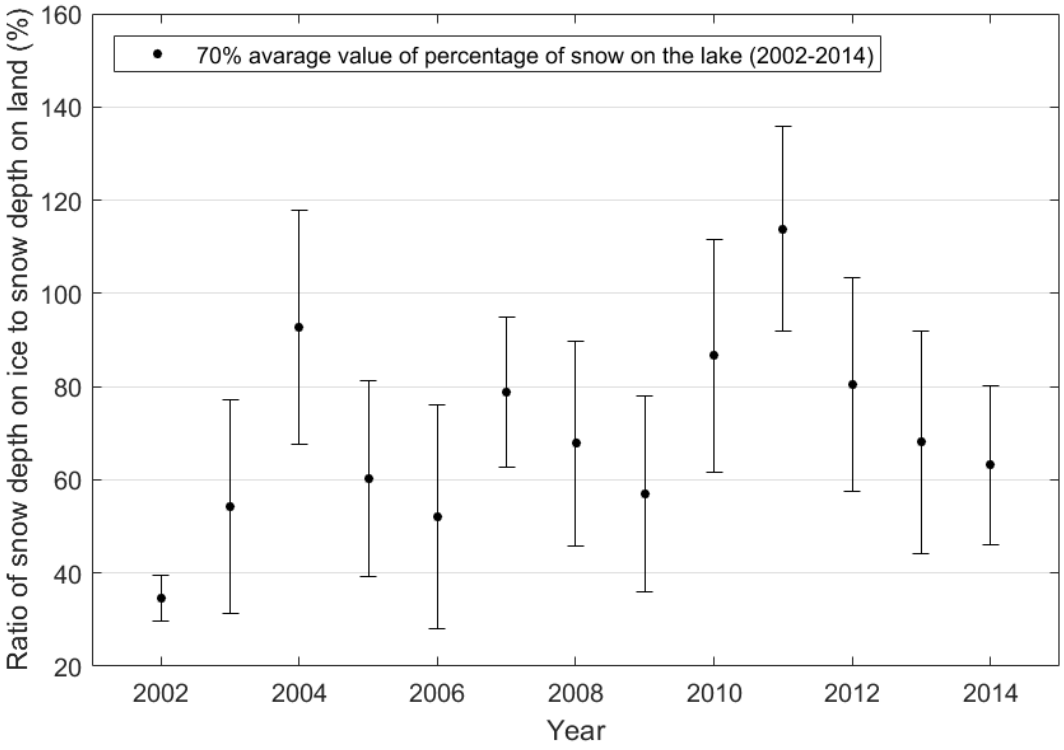
70% avarage value of percentage of snow on the lake (2002-2014)
Ratio of snow depth on ice to snow depth on land (%)
160
140
120
100
80
60
40
20
2002
2004
2006
2008
2010
2012
2014
Year

Fig. 2

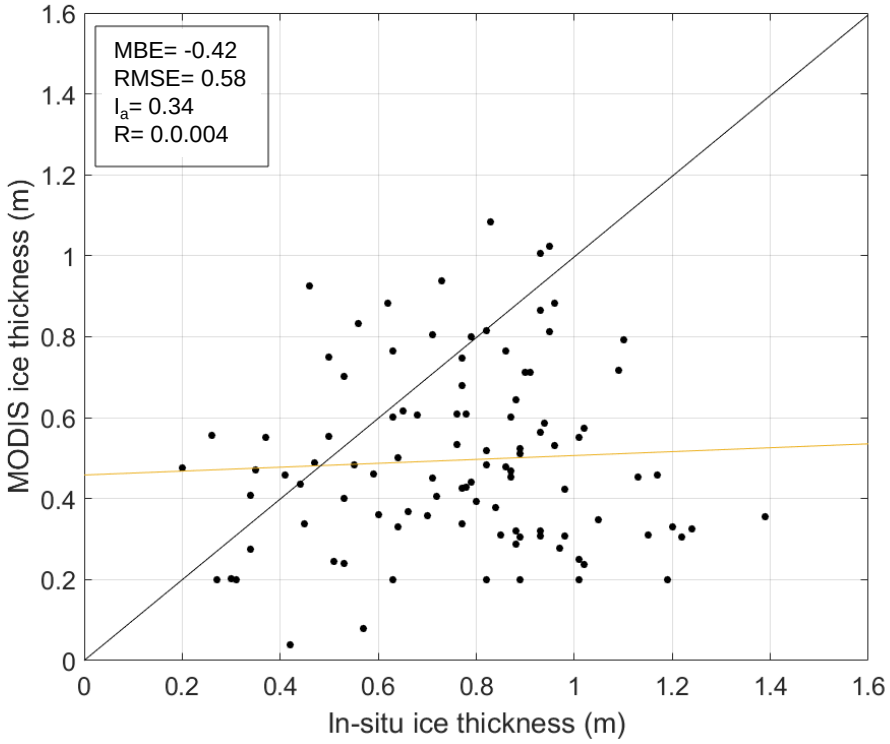
MBE= -0.42
RMSE= 0.58
I_a= 0.34
R= 0.0.004
MODIS ice thickness (m)
In-situ ice thickness (m)
0
0.2
0.4
0.6
0.8
1
1.2
1.4
1.6

Fig. 3

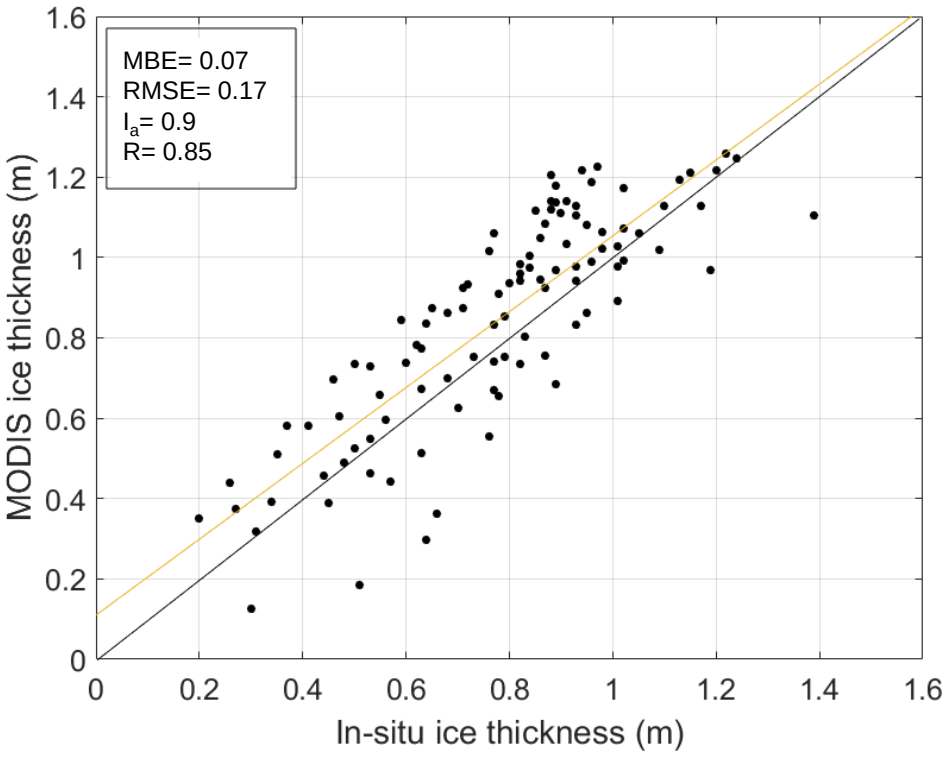
MBE= 0.07
RMSE= 0.17
I_a= 0.9
R= 0.85
MODIS ice thickness (m)
In-situ ice thickness (m)
0
0.2
0.4
0.6
0.8
1
1.2
1.4
1.6

Fig. 4

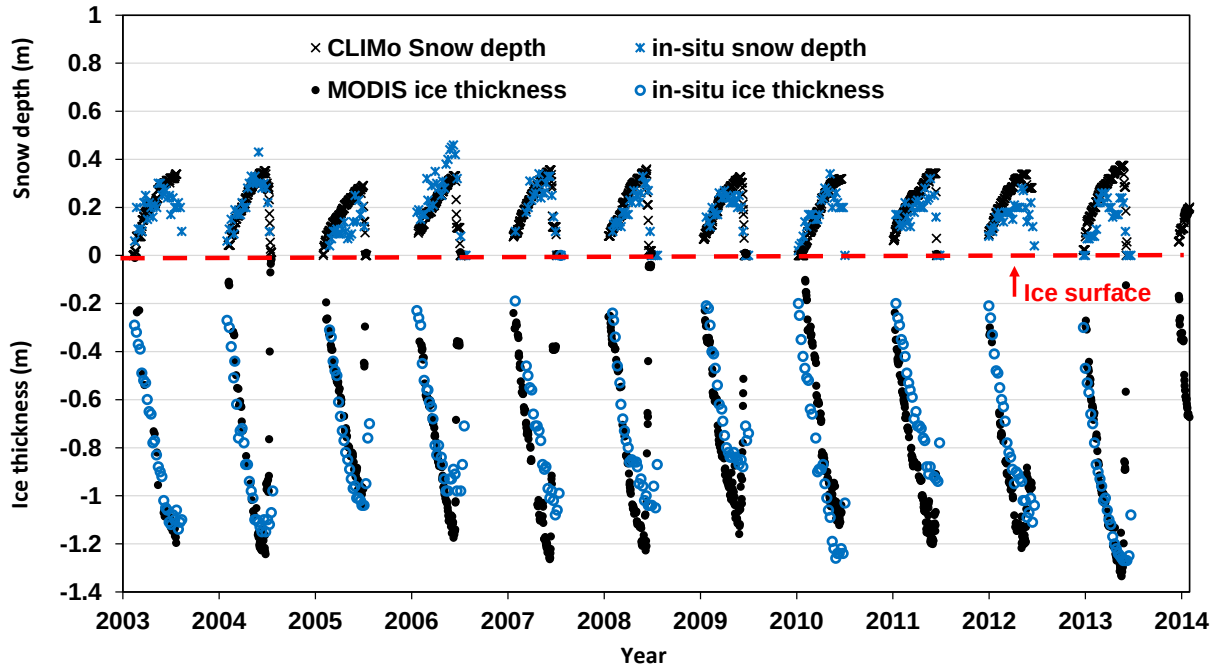
CLIMo Snow depth
in-situ snow depth
MODIS ice thickness
in-situ ice thickness
Snow depth (m)
Ice thickness (m)
Ice surface
Year
1
0.8
0.6
0.4
0.2
0
-0.2
-0.4
-0.6
-0.8
-1
-1.2
-1.4
2003
2004
2005
2006
2007
2008
2009
2010
2011
2012
2013
2014

Fig. 5

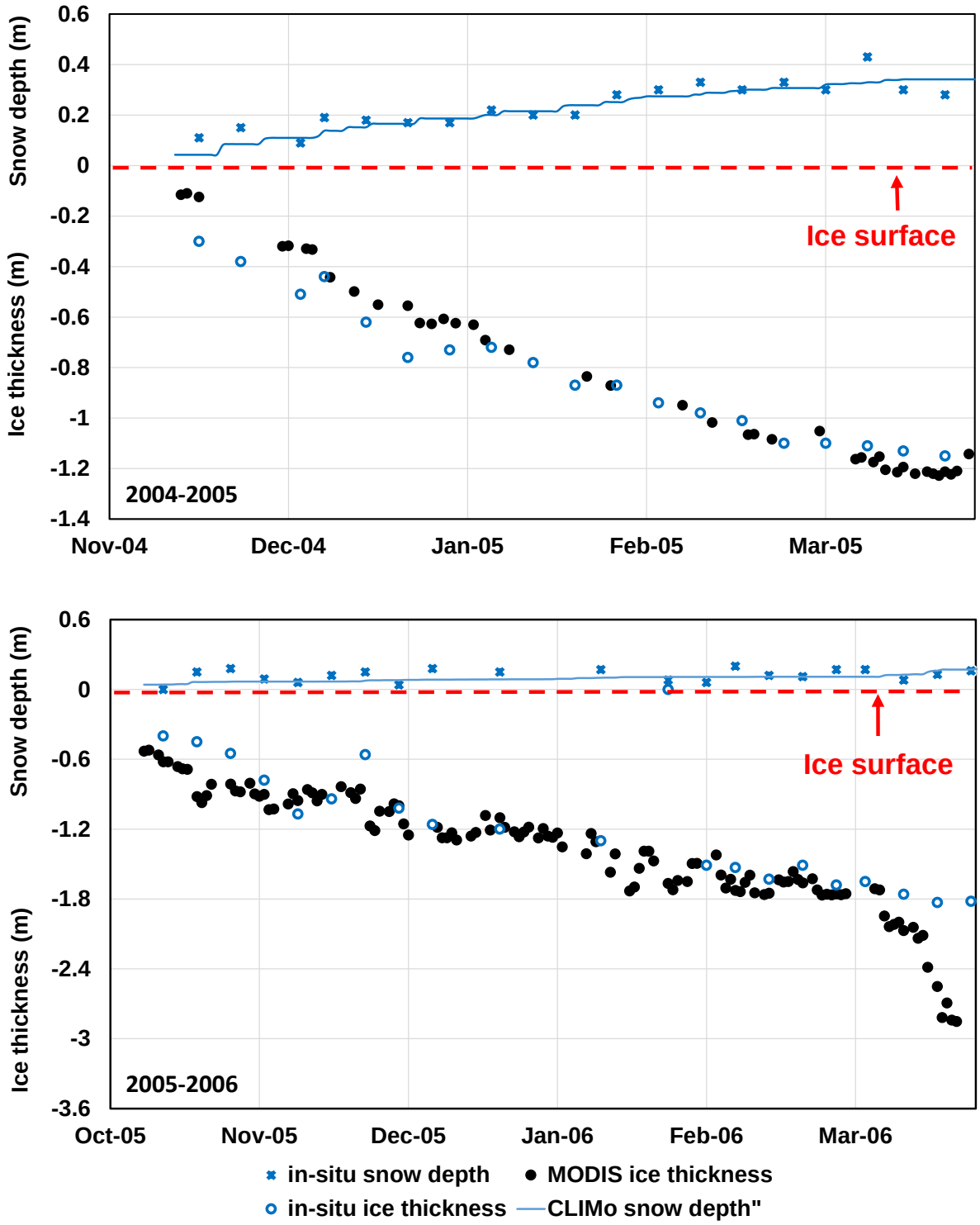
Snow depth (m)
Ice thickness (m)
0.6
0.4
0.2
0
-0.2
-0.4
-0.6
-0.8
-1
-1.2
-1.4
Ice surface
2004-2005
Nov-04
Dec-04
Jan-05
Feb-05
Mar-05
Snow depth (m)
Ice thickness (m)
0.6
0
-0.6
-1.2
-1.8
-2.4
-3
-3.6
Ice surface
2005-2006
Oct-05
Nov-05
Dec-05
Jan-06
Feb-06
Mar-06
in-situ snow depth
MODIS ice thickness
in-situ ice thickness
CLIMo snow depth"

Fig. 6

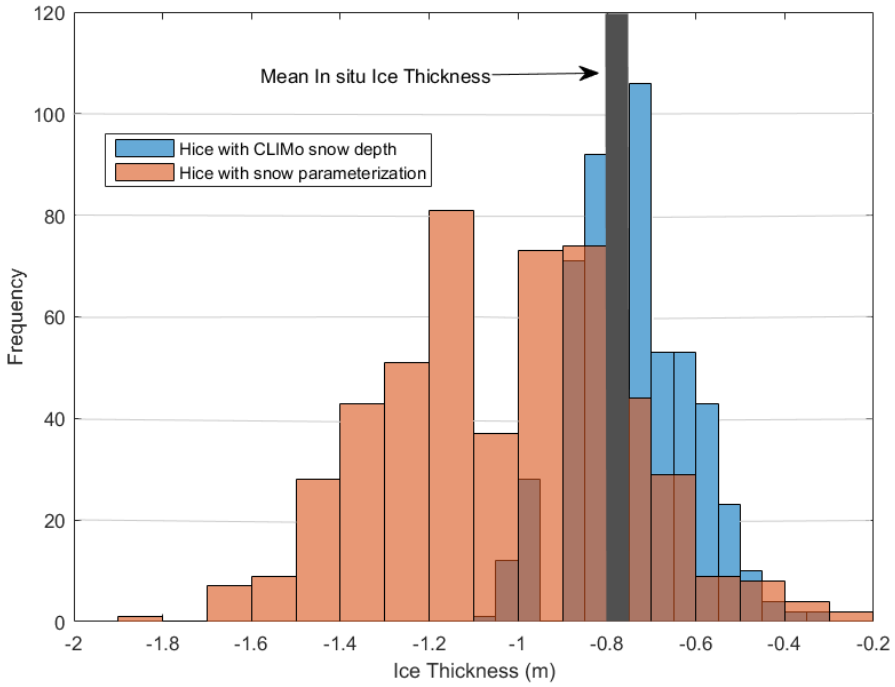
Mean In situ Ice Thickness
Hice with CLIMo snow depth
Hice with snow parameterization
Frequency
Ice Thickness (m)
120
100
80
60
40
20
0
-2
-1.8
-1.6
-1.4
-1.2
-1
-0.8
-0.6
-0.4
-0.2

Fig. 7